JOURNAL OF GEOPHYSICAL RESEARCH, VOL. 113, D16S29, doi:10.1029/2007JD008815, 2008

Validation of Tropospheric Emission Spectrometer ozone profiles with aircraft observations during the Intercontinental Chemical Transport Experiment–B

Nigel A. D. Richards,[1,2] Gregory B. Osterman,[1] Edward V. Browell,[3] Johnathan W. Hair,[3] Melody Avery,[3] and Qinbin Li[1]

Received 15 April 2007; revised 25 October 2007; accepted 17 December 2007; published 23 May 2008.

[1] The Tropospheric Emission Spectrometer (TES) is an infrared instrument that was launched on board NASA's Aura satellite in 2004. TES is the first instrument to provide vertical information on tropospheric ozone while simultaneously measuring CO on a global basis. Before they may be used for scientific study, TES profiles must first be validated to determine if there are any systematic biases present. In this study we present a validation of TES tropospheric ozone using airborne differential absorption lidar (DIAL) profiles obtained during the Intercontinental Chemical Transport Experiment–B (INTEX-B) campaign, which took place during March–May 2006. During INTEX-B the NASA DC-8 aircraft conducted several flights, which allowed the DIAL instrument to obtain ozone profile measurements that were spatially coincident with TES special observations in three different geographical regions. Here we present comparisons of TES and DIAL tropospheric ozone profiles that show that, on average, TES exhibits a small positive bias in the troposphere of 5–15%. We also examine the use of in situ profile observations for the validation of TES tropospheric ozone, and we find these to be of most use in clean regions where the background ozone field is homogeneous.

Citation: Richards, N. A. D., G. B. Osterman, E. V. Browell, J. W. Hair, M. Avery, and Q. Li (2008), Validation of Tropospheric Emission Spectrometer ozone profiles with aircraft observations during the Intercontinental Chemical Transport Experiment–B, *J. Geophys. Res.*, *113*, D16S29, doi:10.1029/2007JD008815.

1. Introduction

[2] Validation of remotely sensed constituent profiles is essential before they may be used for scientific studies. Validation seeks to identify and characterize any systematic biases and random errors that may be present in the reported mixing ratio profile. Validation is conducted through comparisons with independent measurements of the same parameters. The validation of tropospheric ozone, which has a large degree both spatial and temporal variability [*Logan*, 1999], requires that these independent measurements be as close to temporally and spatially coincident with the satellite observations as possible. For this reason, quantifying biases in satellite data is often difficult owing to the paucity of measurements with which to conduct statistically significant comparisons.

[3] The Tropospheric Emission Spectrometer (TES) was designed to provide simultaneous vertical information on tropospheric ozone, CO and other trace gases on a global basis [*Beer et al.*, 2001; *Beer*, 2006]. To date, TES tropospheric ozone validation has been conducted through comparisons with ozonesondes [*Worden et al.*, 2007; *Nassar et al.*, 2008], which are able to make in situ observations from the surface to the stratosphere. Although ozonesondes are able to provide a measurement set which has a large geographical extent, the frequency of ozonesonde launches is quite low, and they are rarely timed to be coincident with satellite overpasses. Therefore, when using ozonesondes, long-timescale analyses and somewhat loose coincidence criteria are required to build sufficient statistics to make meaningful comparisons [*Nassar et al.*, 2008]. Intensive aircraft measurement campaigns however are able to provide a set of high-frequency measurements which are targeted to be coincident with satellite overpasses, albeit on a limited spatial scale. In this work we conduct comparisons between TES Version 2 (V002) tropospheric ozone profiles [*Osterman et al.*, 2006] and data obtained by the differential absorption lidar (DIAL) and the fast response ozone (FASTOZ) instruments during the Intercontinental Chemical Transport Experiment–B (INTEX-B) aircraft campaign (http://www.espo.nasa.gov/intex-b/), which took place in spring 2006. The campaign provided a large number of measurements which were designed to be coincident with TES observations. Using this data set we characterize the bias of TES V002 nadir

[1] Jet Propulsion Laboratory, California Institute of Technology, Pasadena, California, USA.
[2] Now at Institute for Atmospheric Science, School of Earth and Environment, University of Leeds, Leeds, UK.
[3] NASA Langley Research Center, Hampton, Virginia, USA.

0148-0227/08/2007JD008815$09.00

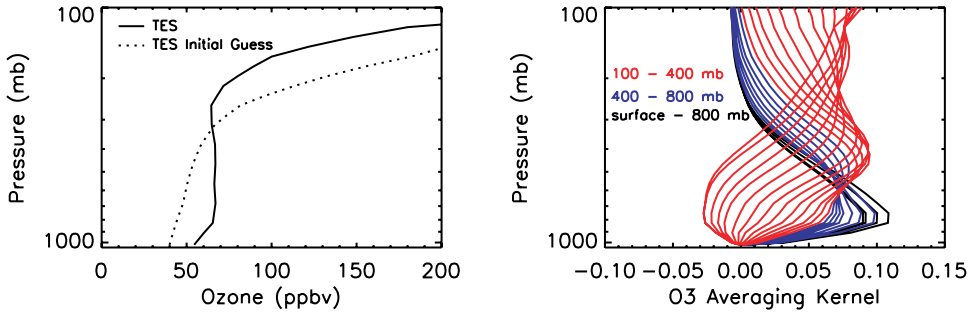

Figure 1. (left) An example of a retrieved Tropospheric Emission Spectrometer (TES) ozone profile obtained on 23 April 2006 close to the Hawaiian Islands. The solid line shows the retrieved profile, and the dotted line shows the initial guess used in the retrieval. (right) The corresponding averaging kernels, where the colors indicate the averaging kernel rows corresponding to the pressure levels in the legend.

ozone profiles over the eastern Pacific and the southern United States.

2. Data

2.1. TES

[4] TES is an infrared Fourier transform spectrometer that measures atmospheric thermal emission over the spectral range 650–2250 cm^{-1}, with a nadir footprint of 5.3 km across track and 8.5 km along track for the 16-detector average [*Beer et al.*, 2001]. TES has two basic science operating modes: global survey and special observations. Global surveys are conducted every other day while special observations are taken as needed in between global surveys. Global surveys taken prior to 21 May 2005 have an along-track nadir sample spacing of 5°, those obtained afterward have an increased nadir sampling of ~1.6° spacing along the orbit track. The analysis presented here utilizes TES version 002 data [*Osterman et al.*, 2006] from both global surveys and step & stare special observations which consist of a series of nadir measurements taken at a spacing of 35 km along the Aura orbit track. TES retrievals utilize an optimal estimation scheme [*Rodgers*, 2000]. An overview of the TES retrieval algorithm and error estimation are discussed by *Bowman et al.* [2002] and *Worden et al.* [2004], and the characterization of errors and vertical information for individual TES profiles are discussed by *Kulawik et al.* [2006]. TES ozone retrievals use a priori information from a climatology developed using the MOZART model [*Brasseur et al.*, 1998; *Park et al.*, 2004]. The vertical resolution of TES nadir ozone profiles is about 6 km in cloud-free conditions [*Bowman et al.*, 2002; *Worden et al.*, 2004]. Figure 1 shows an example of a TES tropospheric ozone profile and the corresponding averaging kernels obtained over the Pacific in April 2006. The retrieved TES profile is significantly different from the initial guess used in the retrieval (below 200 mbar), indicating that in this case TES has sensitivity throughout most of the troposphere. This can also be observed by examining the averaging kernels for the retrieval, there are two distinct groupings of averaging kernels, in fact the averaging kernels exhibit 1.8 degrees of freedom for signal in the troposphere (below 100 mbar), indicating that TES is able to resolve lower and upper tropospheric ozone.

2.2. DIAL Lidar

[5] The NASA Langley airborne differential absorption lidar (DIAL) system [*Richter et al.*, 1997; *Browell et al.*, 1998] makes simultaneous O_3 and aerosol backscatter profile measurements with four laser beams: two in the ultraviolet (UV) for O_3 and one each in the visible and infrared for aerosols. For tropospheric O_3 DIAL measurements, one of the lasers is tuned to an "on-line" wavelength of 289 nm in the Hartley-Huggins absorption band of ozone while the other is tuned to an "off-line" wavelength of 300 nm near the edge of this absorption band. Differences between the lidar return signals at 289 and 300 nm are primarily due to the absorption by ozone as a function of range, and thus a profile of ozone can be determined by examining the relative amount of energy absorbed between the on- and off-line wavelengths as a function of range. DIAL makes measurements in both the nadir (below the aircraft) and in the zenith (above the aircraft) which are combined to construct a complete profile. The vertical resolution of DIAL is 300 m in the nadir and 600 m in the zenith. DIAL is unable to measure ozone at the aircraft altitude or in close proximity to it, so this part of the profile is estimated by interpolating between the nadir and zenith O_3 profiles by using a third-order polynomial least squares fit that is constrained to pass through the in situ O_3 value measured on the DC-8 by FASTOZ (see section 2.3) [*Browell et al.*, 1996]. The airborne DIAL system has been used in many tropospheric chemistry studies including recent investigations of O_3 and aerosols during the TRACE-P (Transport and Chemical Evolution over the Pacific) [*Browell et al.*, 2003a] and TOPSE (Tropospheric Ozone Production about the Spring Equinox) [*Browell et al.*, 2003b] field experiments. Figure 2 shows an example of DIAL ozone measurements together with the corresponding error profiles obtained during an INTEX-B flight.

2.3. FASTOZ

[6] The fast response ozone (FASTOZ) instrument measures in situ ozone along the aircraft flight path. It is capable of fast (1 Hz), sensitive ozone measurements over a large dynamic range and a wide variety of atmospheric

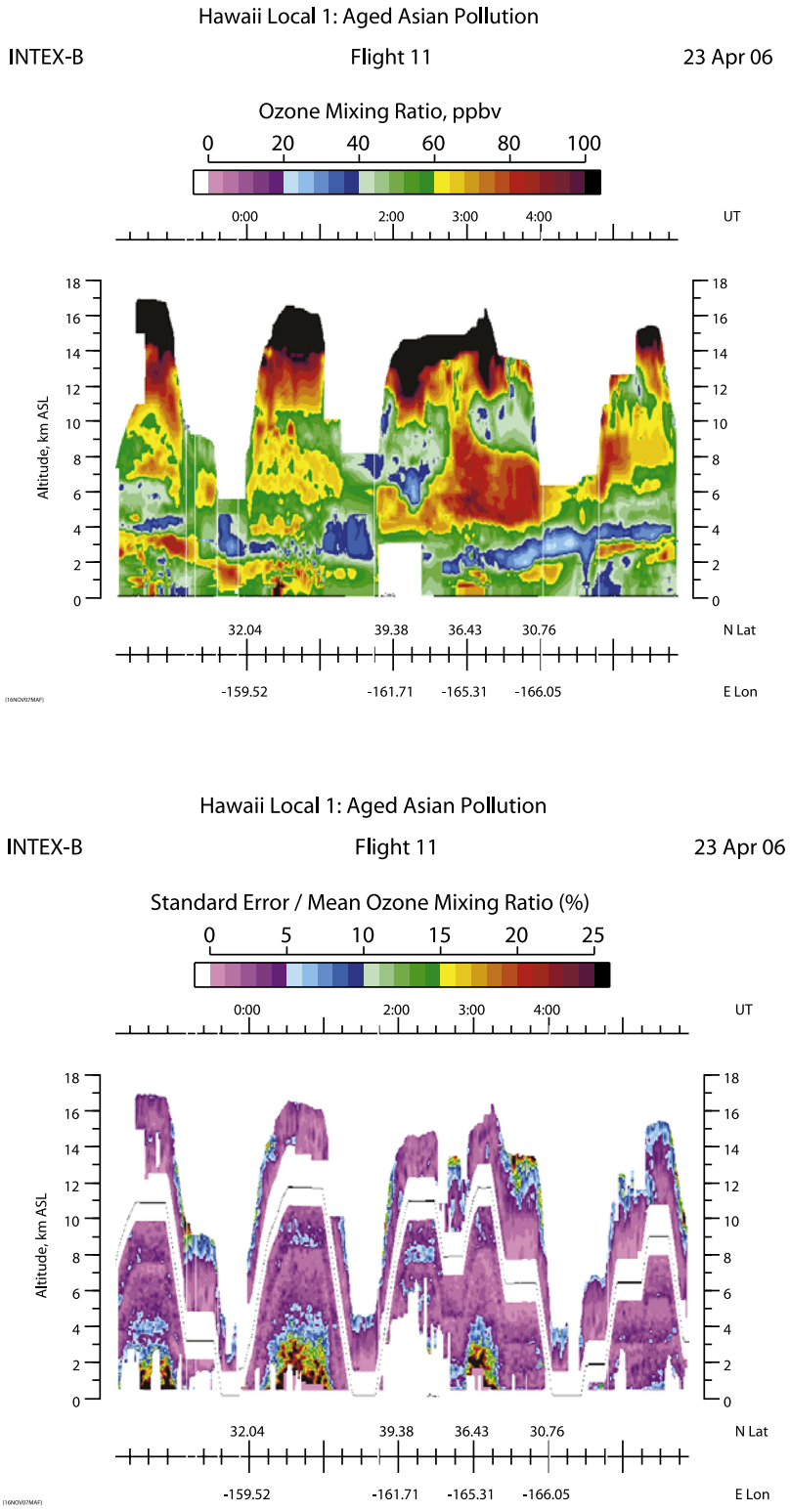

Figure 2. An example of differential absorption lidar (DIAL) (top) ozone observations and (bottom) standard errors, for a flight conducted during Intercontinental Chemical Transport Experiment–B (INTEX-B).

conditions. FASTOZ measures ozone by combining pure reagent nitric oxide (NO) with the incoming air sample in a small volume reaction chamber, and measuring the light from the resulting NO_2 chemiluminescence. The instrument is calibrated by referencing to the NIST standard ozone photometer. The technique, as adapted for use on aircraft, is described in detail by *Eastman and Stedman* [1977], *Gregory et al.* [1987], and *Pearson and Stedman*

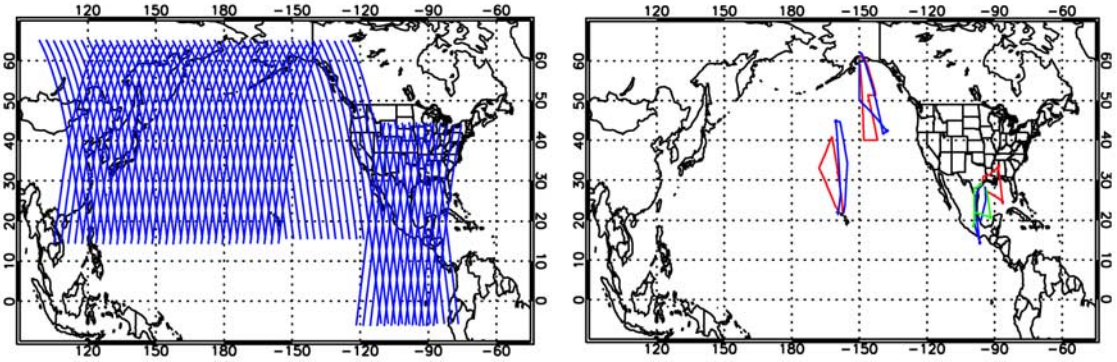

Figure 3. Locations of (left) TES step & stare observations and (right) INTEX-B flight paths, for the period of 1 March to 15 May 2006.

[1980]. FASTOZ ozone concentrations have an estimated uncertainty of 3 ppb or 3% of measured value in dry air, approximately 5–7% in moist air.

3. INTEX-B Campaign

[7] The Intercontinental Chemical Transport Experiment–B (INTEX-B) was an intensive aircraft campaign that took place over a 10-week period from 1 March to 15 May 2006 (http://www.espo.nasa.gov/intex-b/). Among the objectives of the campaign were to observe Mexico City pollution outflow and the transport of Asian pollution to the United States, as well as obtaining temporally and spatially coincident measurements of trace gas species for the validation of remote-sensing instruments on the AURA satellite platform. Measurements were made using NASA's DC-8 aircraft with a range of in situ and remote-sensing instruments. The campaign was split into two phases, during the first phase, performed in March 2006, the DC-8 was based in Houston, Texas, where it conducted a number of flights over the Gulf of Mexico, in the hope of observing the outflow of pollution from Mexico City. The second phase took place during April and May 2006 with the objective of observing Asian pollution outflow over the Pacific. During the second phase the DC-8 conducted several flights out of Honolulu, Hawaii, and Anchorage, Alaska.

[8] During the course of the INTEX-B campaign TES made 243 step & stare special observations over the United States, East Asia, and the Pacific (see Figure 3) in order to try and set a context for the limited spatial extent covered by the aircraft observations. Of the flights conducted, seven were coincident or near-coincident with TES step & stare observations, 3 in Houston, 2 in Hawaii, and 2 in Alaska, the flight tracks for these flights are also shown in Figure 3. These flights each included a sector in which the aircraft flew along the TES orbital track in order to get coincident DIAL observations, and also several spiral maneuvers around TES measurement locations, which enabled the FASTOZ in situ instrument to make measurements of the ozone vertical profile for comparison with TES observations.

4. Comparison Strategy

[9] In order to compare profiles obtained from a remote-sensing instrument such as TES with in situ data, we must first take into account the limited vertical resolution and the affects of a priori information inherent in the retrieved profiles. Averaging kernels (**A**) intrinsically account for both, and together with the a priori profile used in the retrieval ($\mathbf{x_a}$) they form the TES operator, which may be used to transform a comparison profile ($\mathbf{x_{comp}}$) into "TES space" [*Rodgers and Connor*, 2003],

$$\mathbf{X_{final}} \equiv \mathbf{x_a} + \mathbf{A}(\mathbf{x_{comp}} - \mathbf{x_a}) \quad (1)$$

yielding a profile ($\mathbf{x_{final}}$) that may be directly compared with TES, such a comparison is not biased by the TES a priori. Each retrieved TES profile has a unique averaging kernel which must be applied to the comparison profile. The application of the TES operator to a comparison profile is described in more detail by *Worden et al.* [2007]. In order to apply TES averaging kernels to the DIAL and FASTOZ profiles, the TES a priori was used to extend each profile to the highest TES pressure level (0.1 mbar). TES averaging kernels for retrievals above 300 mbar may have some influence from the stratosphere, and since we use the TES a priori for the stratosphere, we cannot be confident of the comparisons above this altitude. Our analysis will therefore be limited to altitudes below 300 mbar, validation of TES

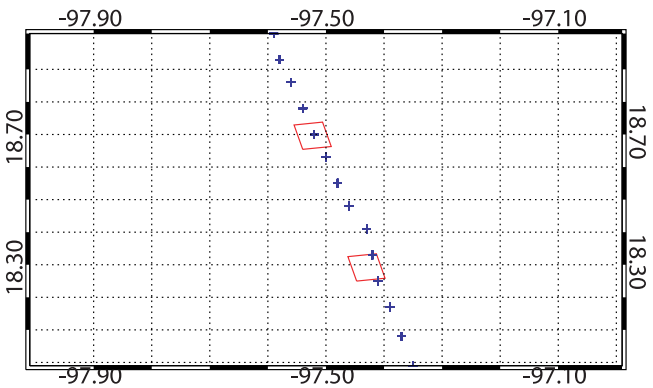

Figure 4. An example of TES and DIAL coincidences during an INTEX-B flight. The red squares indicate the TES measurement footprints, and the blue crosses represent the DIAL observations.

Table 1. Dates and Locations of INTEX-B Flights, Which Include a Flight Leg Along the TES Overpass, Together With the Number of Coincident TES and DIAL Profiles for Each

Date	TES Run ID	Location	Number of Coincidences
4 Mar 2006	3399	Houston	15
12 Mar 2006	3440	Houston	16
16 Mar 2006	3459	Houston	16
23 Apr 2006	3830	Hawaii	39
25 Apr 2006	3868	Hawaii	46
7 May 2006	4112	Anchorage	49
9 May 2006	4154	Anchorage	44
Total			225

ozone above 300 mbar has been conducted using ozonesondes which show no significant bias [*Nassar et al.*, 2008].

4.1. DIAL

[10] All DIAL observations within the footprint of each TES observation were selected and averaged for comparison with the corresponding TES profile. Generally, there are one or two DIAL profiles per TES footprint (see Figure 4). In this study we impose no time coincidence criteria as all aircraft measurements were taken within 3 hours of the satellite overpass, the implications of this will be described later. DIAL profiles were interpolated to the TES pressure grid and each individual TES operator was applied to the resulting profile. When comparing TES and DIAL profiles, those pressure levels at which a priori information was used are discounted from the analysis as are any profiles that failed the TES quality control, as indicated by the TES quality flags [*Osterman et al.*, 2006]. Table 1 shows the dates of the seven INTEX-B flights which are coincident with TES overpasses, together with the number of coincident TES profiles per flight. In total there are 225 coincident TES and DIAL profiles which are used in this analysis.

4.2. FASTOZ

[11] Each FASTOZ profile is constructed by taking all FASTOZ measurements obtained during an aircraft spiral maneuver, the observations are then interpolated onto the TES pressure grid and the TES operator applied. Each spiral was targeted so as to be temporally coincident with a TES observation and was centered on a TES measurement point

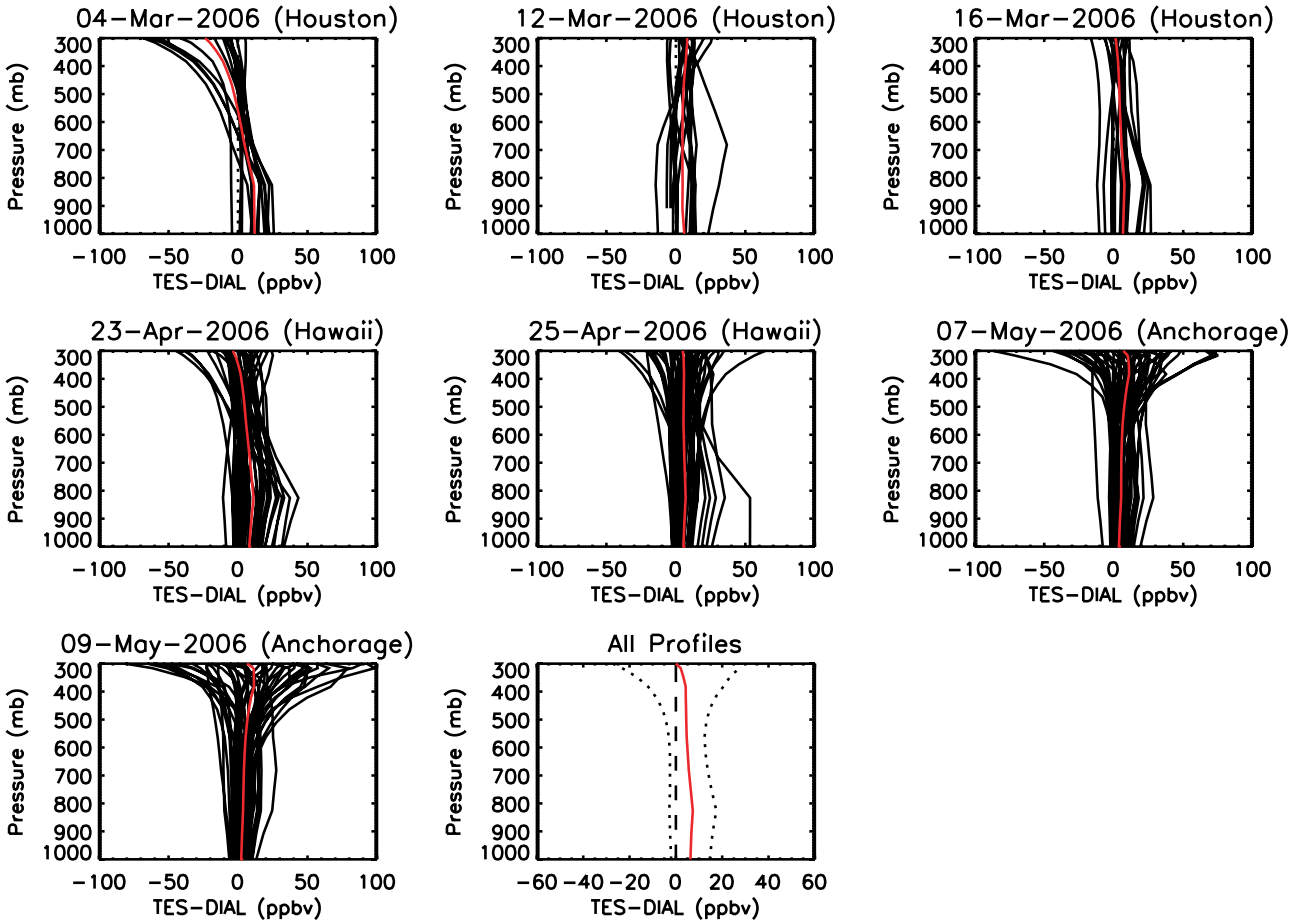

Figure 5. Ozone difference profiles for the seven individual coincident INTEX-B flights and mean difference profile for all flights. The black lines in each plot represent the differences for the individual profiles, and the red lines indicate the mean. The dotted lines on the mean difference plot for all flights (last plot) indicate plus and minus one standard deviations.

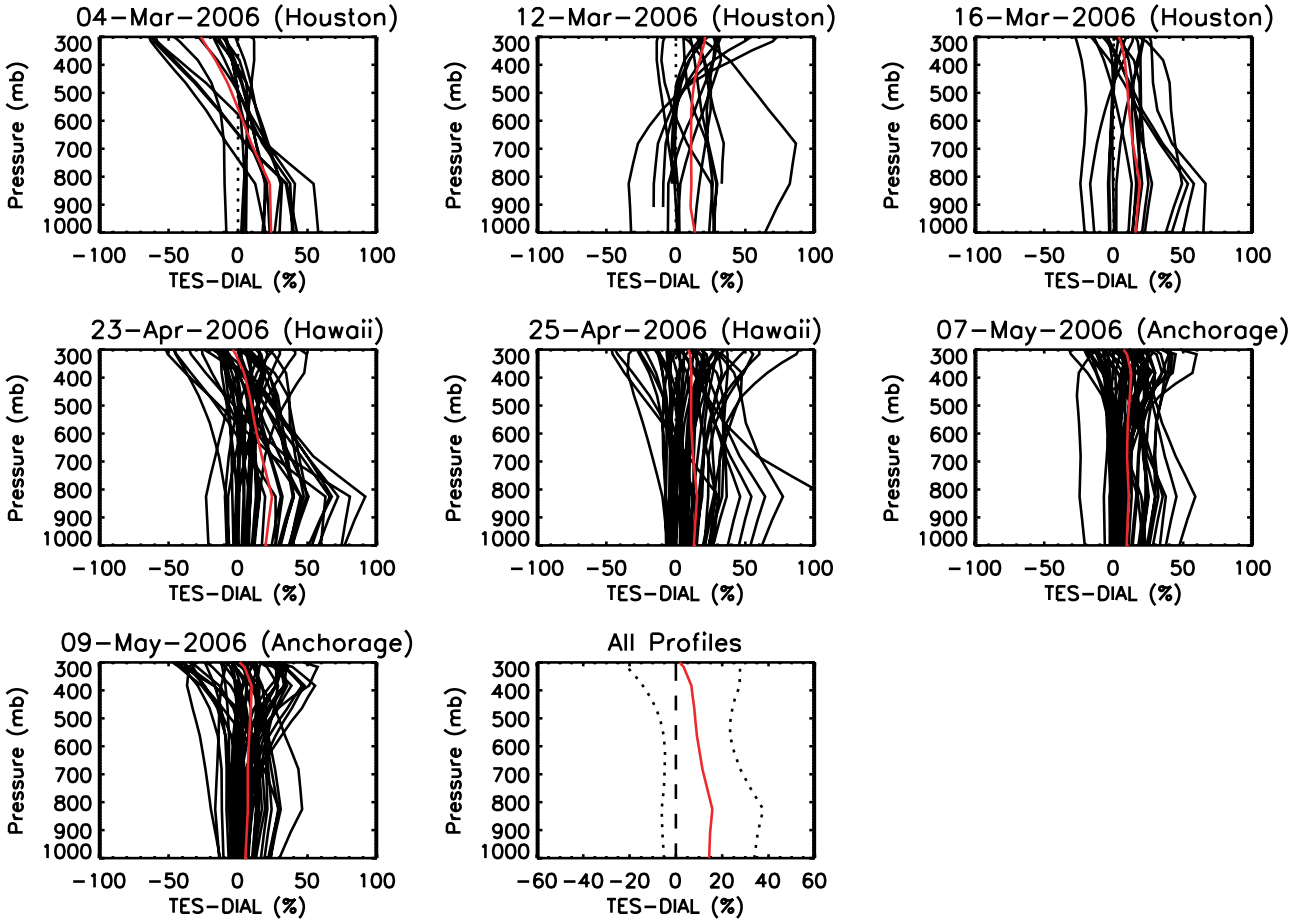

Figure 6. The same as Figure 5 but represented as percentage differences relative to DIAL.

for comparison. In total, for the INTEX-B campaign there were 14 such comparison profiles.

5. Results

5.1. DIAL

[12] Figures 5 and 6 show ozone difference profiles in ppbv and percent, respectively, for all seven INTEX-B coincident flights, together with the mean difference for all flights. Individual profiles are plotted in black with the mean differences overlaid in red. The dotted lines in the mean difference plot indicate the one standard deviation range.

[13] Over all flights DIAL and TES compare very well, with a mean difference between the two of less than 20%. In the middle and lower troposphere TES exhibits a small positive bias relative to DIAL, which remains fairly constant at about 7 ppbv throughout the troposphere. In percentage terms the bias is seen as a 15% positive bias at the surface, which falls with increasing altitude to around 5% at 300 mbar. These findings are consistent with the latest TES validation study using ozonesondes [*Nassar et. al.*, 2008].

[14] Larger differences are observed in the Houston region where the air was relatively clean over the Gulf of Mexico compared to the other locations, and this could be due to a lower signal from which to retrieve TES profiles. There were also fewer coincident profiles with which to make comparisons as the TES validation flight legs were shorter in this region. The differences for Hawaii and Anchorage exhibit a larger degree of variability, particularly Hawaii, this likely reflects variability in the ozone concentrations due to the long-range transport of pollution from Asia. Despite the variability, the mean differences between TES and DIAL remain quite small; this suggests that TES is able to capture some of the observed variability in these regions. The higher ozone concentrations in these regions will also contribute to the quality of the comparison, since TES sensitivity increases with increasing ozone concentration.

[15] Since TES ozone profiles generally exhibit only two degrees of freedom in the troposphere, we have split the data into two altitude regions for analysis. For this study, the lower altitude region is defined as the surface to 500 mbar and the upper region as 500 mbar to 300 mbar. Figure 7 shows probability density function (PDF) plots of TES-DIAL ozone differences, and Table 2 shows the correlation, bias, and standard deviation for the two altitude regions for each of the three INTEX-B geographical regions being considered. The PDFs for all regions exhibit a general Gaussian shape with biases of less than 10 ppbv. The biases for the upper and lower altitude regions in Hawaii are 3.11 and 6.89 ppbv, respectively. The upper level Hawaiian PDF has almost a double peak which is due to some of the data points in this region being in the stratosphere. By examining

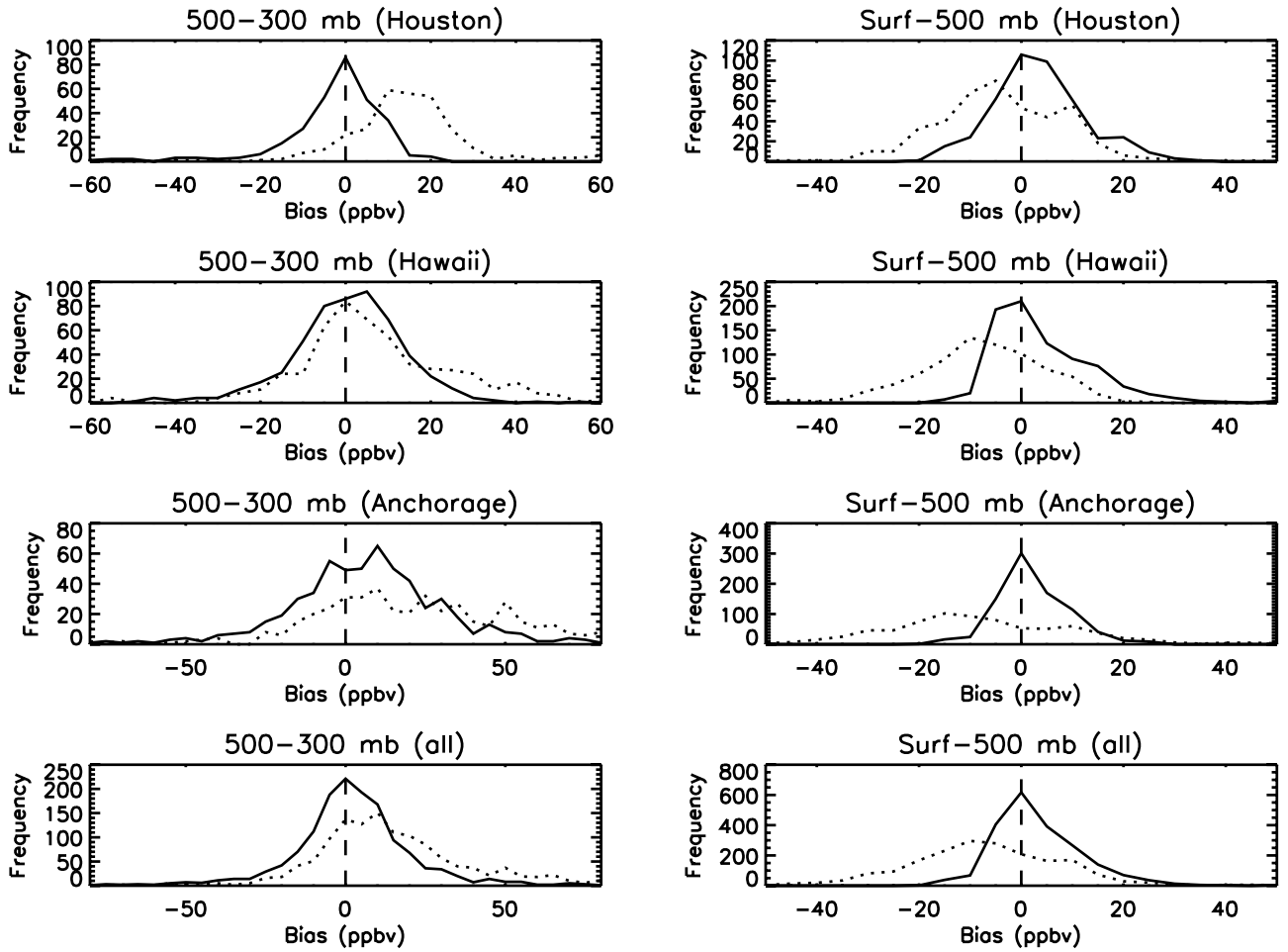

Figure 7. Probability density function plots showing the absolute differences between TES and DIAL ozone (solid lines) for two vertical regions (surface to 500 mbar and 500–300 mbar) for the three different INTEX-B regions and the overall differences for the campaign. The dotted lines indicate the differences between the TES a priori and the DIAL ozone profiles. The dashed lines show the zero bias line.

the individual DIAL profiles (Figure 8), it is possible to see that the poor correlations observed in Hawaii may be due to the large degree of variability in tropospheric ozone over this region. Houston also exhibits low correlations for both the lower and upper altitudes with biases of 5.93 and −1.19 ppbv, respectively. Again this is likely due to the variability of tropospheric ozone in this region observed by DIAL. For Anchorage the correlations are excellent for both altitude regions, and the TES data exhibits a bias of 4.71 and 9.05 ppbv in the lower and upper altitude bands, respectively. There is a double peak in the PDF for the 500–300 mbar band for Anchorage; the negative peak observed in this distribution is due to the low tropopause in this region, and therefore a significant amount of stratospheric air is present in the comparisons. One reason for the excellent correlation in the lower troposphere compared to the other locations might be that tropospheric ozone in this region exhibits a smaller degree of variability as observed by DIAL. By examining all three regions it would seem that the best comparisons are observed in the polluted middle and upper troposphere, and that TES exhibits a small negative bias in the lower stratosphere.

[16] One reason for some of the observed differences could be the temporal displacement of the observations. In this study we used no time coincidence criteria since the aircraft observations target the TES overpass. However, the TES overpass occurs in a matter of minutes, whereas the aircraft can take up to 3 hours to complete its measurement run. This time difference could lead to TES and DIAL measuring very different air masses owing to the movement of the air during this time. The amount of movement of the air between when TES makes a measurement and the time it takes the aircraft to reach the same location, depends on the meteorology at the measurement location, and the altitude at which the comparison is being made. Table 3 shows the results of a trajectory analysis for the seven INTEX-B flights. In this exercise we assume the maximum time difference between TES and DIAL observations is 3 hours, we then run 3 hour forward trajectories from the TES observation locations at three different altitudes to determine the maximum likely distance which separates the air masses measured by the two instruments. It can be seen that depending on the location, altitude and meteorology there can be significant movement of the air, effectively displacing

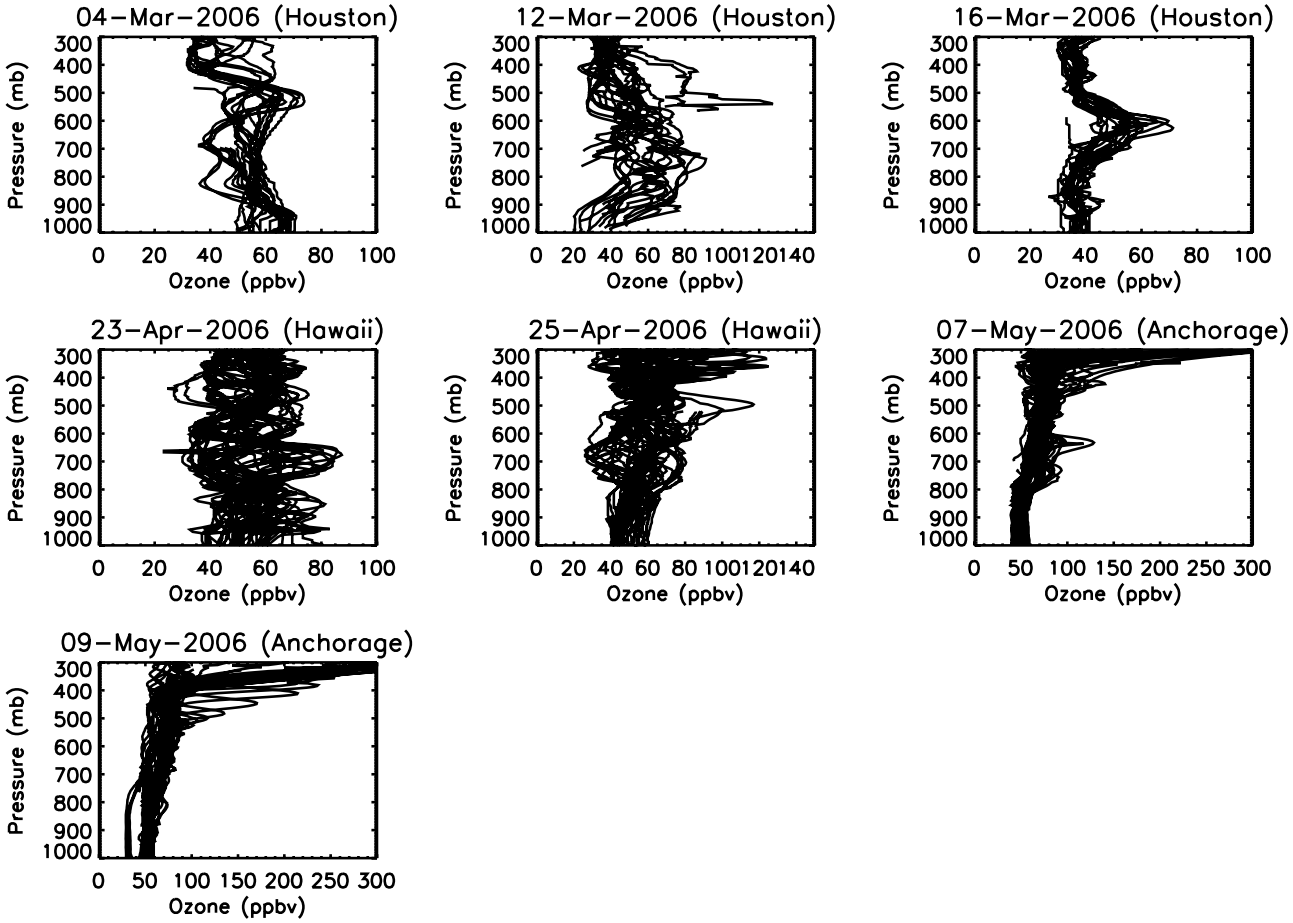

Figure 8. All DIAL ozone profiles used in the comparisons for each of the seven validation flights.

the measurements of the two instruments by up to 500 km. Figure 9 shows full flight cross sections of ozone for each of the flights as observed by DIAL. It can be seen from these plots that tropospheric ozone can be very variable, depending on location, and can exhibit a large degree of fine-scale structure. This is particularly evident in the Hawaiian region, which is also where we observe a large degree of variability in TES-DIAL differences. Alaska, however, has a more homogeneous ozone field and this is reflected in a lower degree of variability in the comparisons, particularly in the lower troposphere. Given the high degree of variability in tropospheric ozone at some locations, it should be noted that these temporal differences may have a large impact on the comparisons.

[17] An examination of MODIS cloud products indicates broken cloud in almost all regions of comparison which might also have an effect on the observed biases. However, TES is also able to measure cloud optical depth, and the reported cloud optical depths for all comparison profiles, except some profiles in Anchorage, are very small. Analysis of the bias as a function of cloud optical depth for the comparison profiles studied here indicates only a small dependence of the TES-DIAL bias on this property, with a reduction in the scatter of the bias as a function of altitude for large optical depths. This is due to a decrease in the degrees of freedom for signal available for the TES retrieval in the presence of thick clouds.

5.2. FASTOZ Spirals

[18] The comparison of in situ aircraft ozone profiles with satellite observations such as TES is difficult owing to the large degree of spatial variability exhibited by tropospheric ozone. In order to construct an ozone profile the aircraft must perform a spiral, and the diameter of the spiral can be quite large, around 2–4 times larger than the TES footprint. During the spiral the FASTOZ instrument obtains only one observation at each altitude, which are then used to construct the profile. The resulting profile may therefore often be pieced together from different air masses which contain

Table 2. Correlation, Bias, and Standard Deviation of the Bias for Each of the Data Sets Shown in Figure 7

Region	Correlation	Bias, ppbv	Standard Deviation, ppbv
Houston (500–300 mbar)	−0.284	−1.19	15.36
Houston (surf–500 mbar)	0.315	5.93	9.14
Hawaii (500–300 mbar)	0.334	3.11	13.65
Hawaii (surf–500 mbar)	0.410	6.89	9.74
Anchorage (500–300 mbar)	0.902	9.05	25.33
Anchorage (surf–500 mbar)	0.879	4.71	6.87

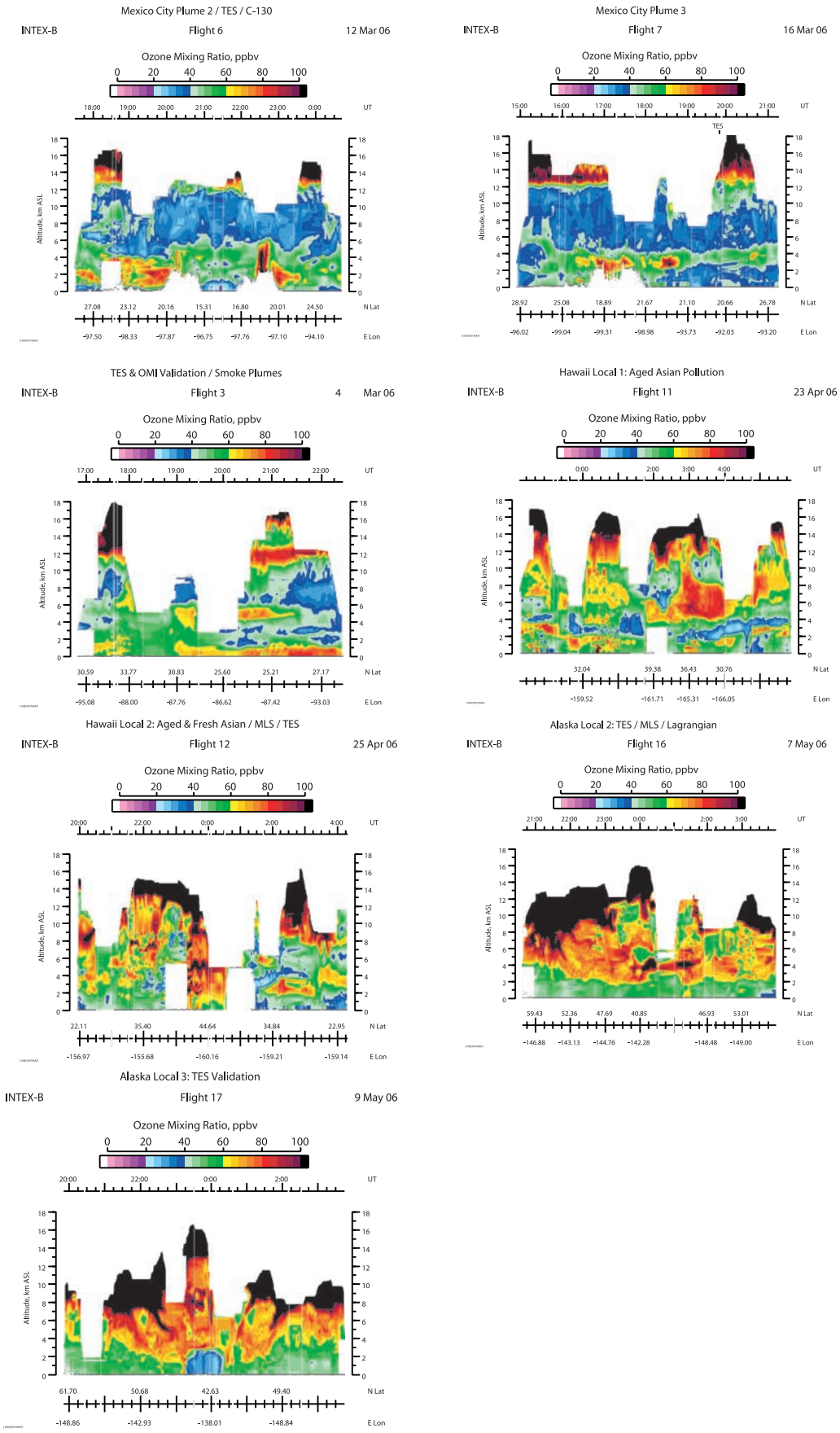

Figure 9. Full ozone cross sections obtained by DIAL for each of the seven flights shown in Figure 3.

Table 3. Maximum Distance Between TES and DIAL "Coincident" Observations Due to Differences in Measurement Times, as Determined by Trajectory Analysis at Three Different Altitudes

Date	TES Run ID	1-km Altitude	5-km Altitude	8-km Altitude
4 Mar 2006	3399	93 km	204 km	254 km
12 Mar 2006	3440	155 km	418 km	517 km
16 Mar 2006	3459	317 km	339 km	333 km
23 Apr 2006	3830	100 km	244 km	425 km
25 Apr 2006	3868	155 km	272 km	390 km
7 May 2006	4112	140 km	250 km	304 km
9 May 2006	4154	302 km	262 km	327 km

very different ozone concentrations, and may not be representative of the average profile over the measurement area. This also complicates the application of the TES averaging kernels since one factor contributing to the sensitivity of TES to ozone at a particular altitude is the ozone concentration itself, and the use of a single averaging kernel for such a region may not be appropriate. An example of this can be seen in Figure 10, which shows a comparison between TES and a FASTOZ profile obtained on 12 March during the Houston phase of INTEX-B. It can be seen from the FASTOZ profile that the aircraft flew through possibly three different ozone regimes. At the bottom of the spiral which covers the southwest quadrant of the region the ozone concentration is around 50 ppbv, as the aircraft approaches the northeast of the region, at around 700 mbar, the ozone concentration jumps to over 70 ppbv for a very short period before dropping to less than 40 ppbv in the east and southeast region. The resulting FASTOZ profile is very complicated and is unlikely to be representative of the whole region. After the TES operator is applied to the FASTOZ profile the high ozone concentrations in the lower troposphere and the low concentrations in the upper troposphere are averaged together to give a rather flat profile with low concentrations throughout the troposphere. There are two TES observations in this region which are separated by just 35 km. Despite the relative proximity of the two profiles, they exhibit very different ozone characteristics. The first TES profile is close to the center of the spiral and exhibits enhanced ozone concentrations throughout most of the troposphere. Whereas the second TES observation, to the northwest, shows a relatively clean background ozone profile, which more closely resembles the transformed FASTOZ profiles. This leads to a large positive mean bias in the TES profiles relative to FASTOZ. This demonstrates how the ozone field can change dramatically over small spatial scales, and highlights the difficulties in making comparisons between TES and in situ observations of this type in such regions.

[19] However, the FASTOZ spiral profiles are useful for validating TES profiles of background ozone concentrations in regions where the ozone field is quite homogeneous. Figure 11 shows an example of such a profile obtained on 9 March during the Houston phase of INTEX-B, where the ozone concentration is around 50 ppbv throughout the whole of the spiral. The TES averaging kernels for this profile exhibit only 1 degree of freedom in the troposphere, with the sensitivity for all levels peaking between 600 and 400 mbar. The resulting FASTOZ profile after the application of the TES operator is very close to the TES profile. In fact TES exhibits only a small positive bias of just 5% throughout the profile up to approximately 300 mbar. This is consistent with the DIAL comparisons reported earlier.

6. Conclusions

[20] During the course of INTEX-B, 225 coincident profiles were obtained by the DIAL instrument for the validation of TES tropospheric ozone. These covered the region of the eastern and central North Pacific and the southern United States. A variety of conditions were observed during these observations, from relatively clean air in the Gulf of Mexico to more polluted air in the northeastern Pacific. On average, TES V002 ozone profiles exhibit a small positive bias of 7 ppbv (5–15%). Larger differences are observed in cleaner regions than in more polluted regions, this is likely due to the reduced signal available for TES to retrieve profile information. Some of the differences may be due to the temporal mismatch of up to 3 hours between the DIAL and TES observations, which trajectory analysis shows can result in an effective spatial separation of up to 500 km. Another factor that complicates the comparison is that the scenes being compared will not be exactly spatially coincident owing to the different field of views of the two instruments, which may lead to representation errors in a nonuniform field.

[21] The use of in situ aircraft observations of ozone for the validation of TES tropospheric profiles is fraught with difficulties. Owing mainly to the large area over which the profiles are obtained, leading to a comparison profile which is often not representative of the whole region over which it is collected. However, FASTOZ spiral observations are useful for validation in remote regions where the background ozone field is quite homogeneous. In such cases comparisons with TES are very good indicating only a small positive bias in the TES observations throughout most of the troposphere, consistent with comparisons of TES and DIAL.

[22] The difficulty in using in situ observations, arising from the spatial scales of tropospheric ozone variability, for satellite validation highlighted here are similar to those faced when conducting comparisons with ozonesonde measurements. One advantage here, however, is that in the case of in situ aircraft measurements of ozone we have geolocation coordinates for each observation. We also have the coincident DIAL lidar profile measurements. By using these two data sets together we are able to characterize the variability of tropospheric ozone in the region of interest. We may therefore be able to make an assessment of the impact of tropospheric ozone variability on the use of in situ aircraft observations for the validation remotely sensed ozone profiles from satellite instruments such as TES. This will be the subject of a future paper, which will include a more extensive comparison of TES and FASTOZ.

7. Recommendations for Future Validation Campaigns

[23] During this study we have found DIAL lidar data to be of great use for the validation of TES tropospheric ozone

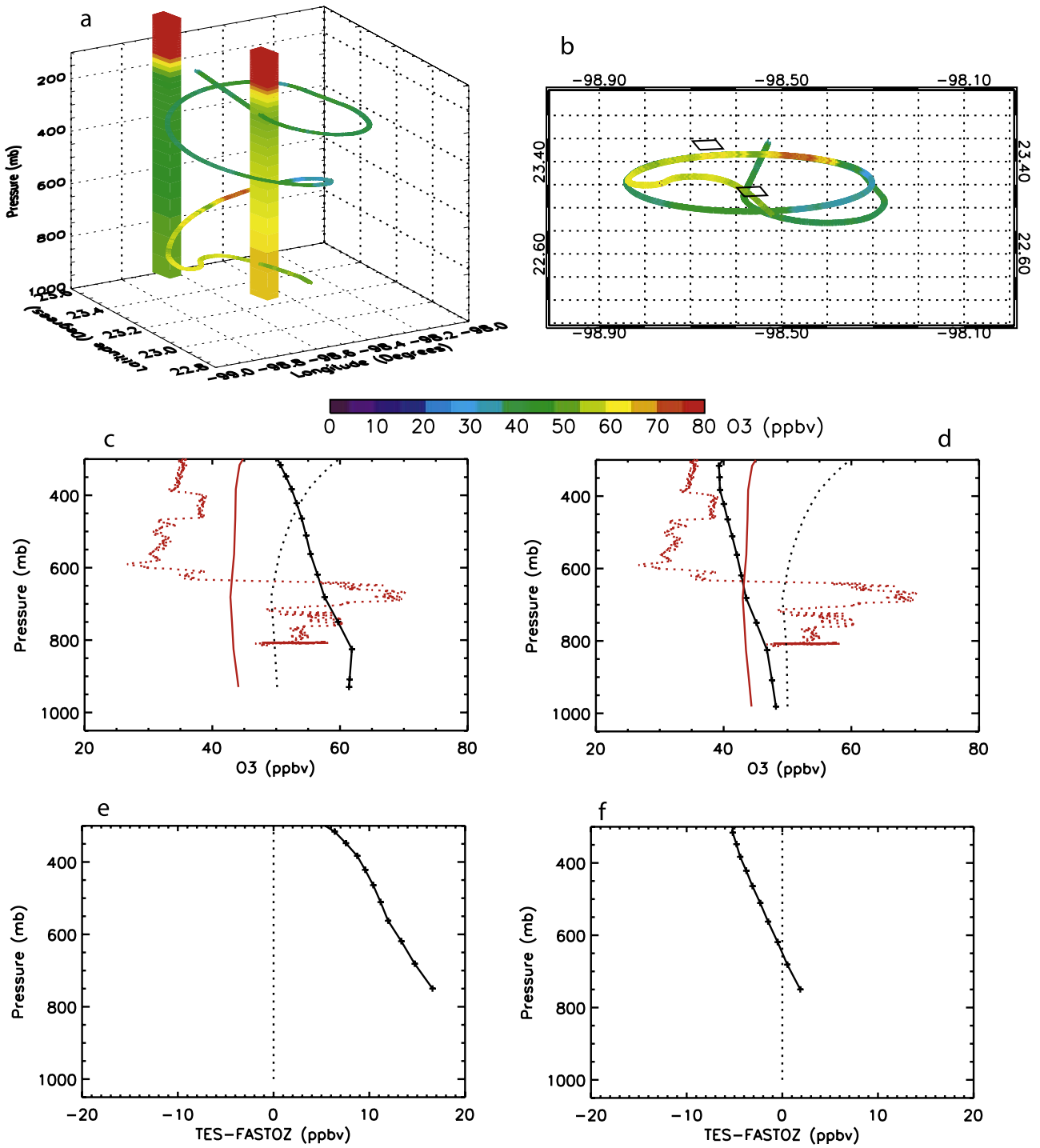

Figure 10. Comparison of fast response ozone (FASTOZ) and TES for a spiral conducted during an INETX-B flight on 12 March 2006. (a) A 3-D representation of the aircraft spiral and the coincident TES profiles. (b) The spiral as viewed from above, where the black lines represent the size and location of the TES footprints. (c, d) Comparisons for the two TES profiles against the FASTOZ profile, where the solid black line indicates the TES profile, the dotted black line indicates the TES a priori profile, the dotted red line is the original FASTOZ profile, and the solid red line is the FASTOZ profile after the application of the TES averaging kernel. (e, f) The difference profiles for the two comparisons.

profiles. This is due mainly to its ability to obtain high-frequency, instantaneous, profile measurements of tropospheric ozone concentrations. In light of some of the findings here, we would like to make two suggestions for consideration in the planning of future tropospheric ozone aircraft validation campaigns using DIAL. First, in order to minimize the time differences between satellite and DIAL observations, we would suggest a time coincident

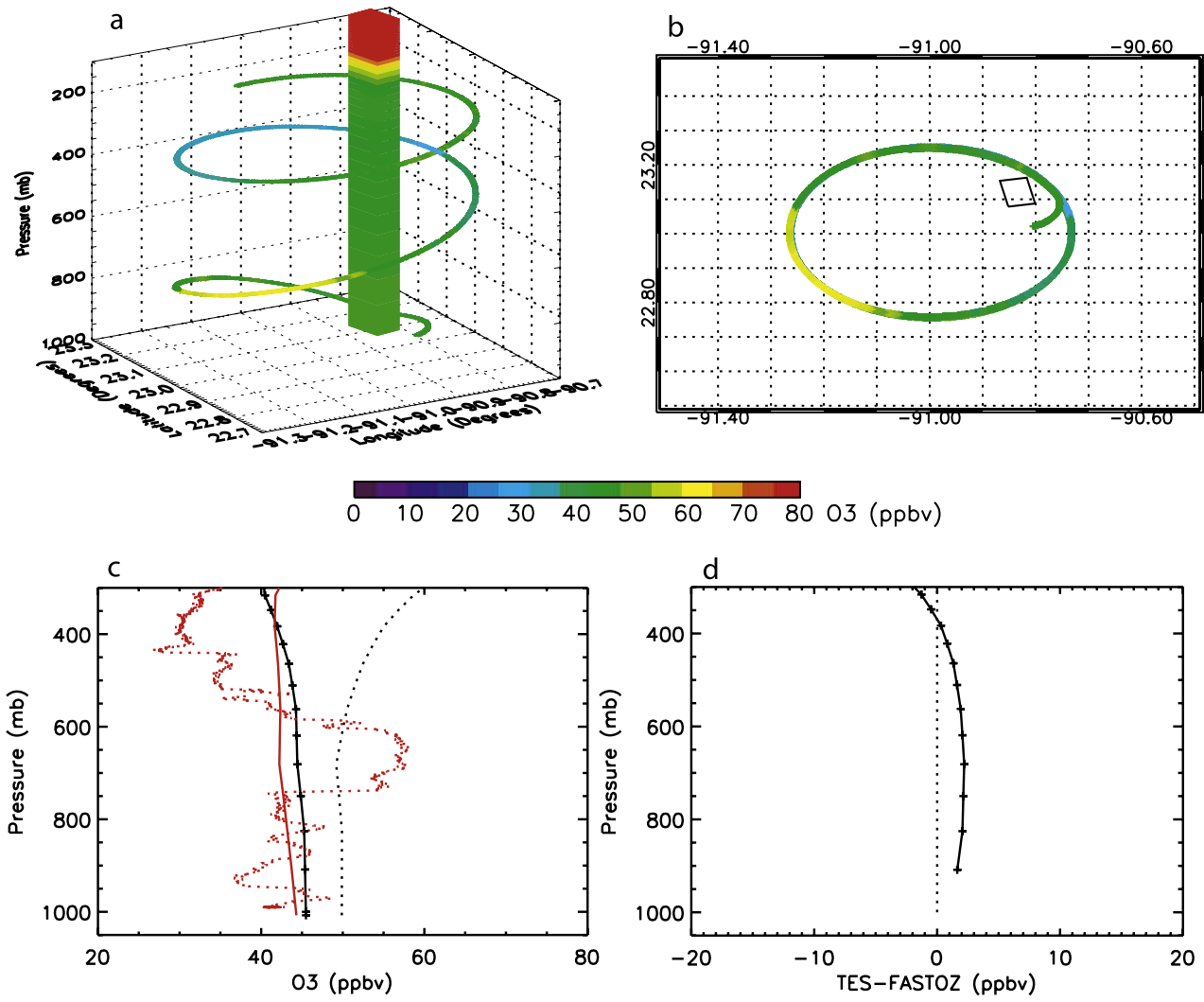

Figure 11. (a–d) Same as Figure 10 for a flight conducted on 9 March 2006, in which there is only one coincident TES profile.

rendezvous point be scheduled for the halfway point of the validation flight leg. Our second suggestion would be the use of forecast trajectories in the planning of the flights. These may be used to offset the flight path from the satellite measurement points to try and account for the movement of air due to time differences in the observations. Inclusion of other instrumentation on the aircraft may also facilitate comparisons, such as a passive infrared Fourier transform spectrometer which would enable better field of view matchups with TES, and allow the observed radiances to be compared directly, thereby helping to separate sensor/algorithm issues. By following these suggestions, we hope that future validation campaigns will be able to minimize the effects of ozone variability and improve the quality of comparisons.

[24] **Acknowledgments.** The authors would like to thank the TES, DIAL, FASTOZ, and INTEX-B teams for their considerable efforts in obtaining and analyzing the ozone data used in this investigation. This work was performed at the Jet Propulsion Laboratory, California Institute of Technology, under contract with NASA.

References

Beer, R. (2006), TES on the Aura mission: Scientific objectives, measurements, and analysis overview, *IEEE Trans. Geosci. Remote Sens.*, *44*(5), 1102–1105.

Beer, R., T. A. Glavich, and D. M. Rider (2001), Tropospheric Emission Spectrometer for the Earth Observing System's Aura satellite, *Appl. Opt.*, *40*, 2356–2367.

Bowman, K. W., T. Steck, H. M. Worden, J. Worden, S. Clough, and C. Rodgers (2002), Capturing time and vertical variability of tropospheric ozone: A study using TES nadir retrievals, *J. Geophys. Res.*, *107*(D23), 4723, doi:10.1029/2002JD002150.

Brasseur, G. P., D. A. Haulgastine, S. Walters, P. J. Rasch, J. F. Muller, C. Granier, and X. X. Tie (1998), MOZART, a global chemical transport model for ozone and related chemical tracers: 1. Model description, *J. Geophys. Res.*, *103*, 28,265–28,289.

Browell, E. V., et al. (1996), Ozone and aerosol distributions and air mass characteristics over the South Atlantic Basin during the burning season, *J. Geophys. Res.*, *101*, 24,043–24,068.

Browell, E. V., S. Ismail, and W. B. Grant (1998), Differential Absorption Lidar (DIAL) measurements from air and space, *Appl. Phys. B*, *67*, 399–410.

Browell, E. V., et al. (2003a), Large-scale ozone and aerosol distributions, air mass characteristics, and ozone fluxes over the western Pacific Ocean in late-winter/early-spring, *J. Geophys. Res.*, *108*(D20), 8805, doi:10.1029/2002JD003290.

Browell, E. V., et al. (2003b), Ozone, aerosol, potential vorticity, and trace gas trends observed at high latitudes over North America from February to May 2000, *J. Geophys. Res.*, *108*(D4), 8369, doi:10.1029/2001JD001390.

Eastman, J. A., and D. H. Stedman (1977), A fast response sensor for ozone eddy-correlation flux measurements, *Atmos. Environ.*, *11*, 1209–1211.

Gregory, G. L., C. H. Hudgins, J. Ritter, and M. Lawrence (1987), In situ ozone instrumentation for 10-Hz measurements: Development and evaluation, paper presented at Sixth Symposium on Meteorological Observations and Instrumentation, Am. Meteorol. Soc., New Orleans, La., 12–16 Jan.

Kulawik, S. S., et al. (2006), TES atmospheric profile retrieval characterization: An orbit of simulated observations, *IEEE Trans. Geosci. Remote Sens.*, *44*(5), 1324.

Logan, J. A. (1999), An analysis of ozonesonde data for the troposphere: Recommendations for testing 3-D models and development of a gridded climatology for tropospheric ozone, *J. Geophys. Res.*, *104*(D13), 16,115–16,149.

Nassar, R., et al. (2008), Validation of Tropospheric Emission Spectrometer nadir ozone profiles using ozonesonde measurements, *J. Geophys. Res.*, *113*, D15S17, doi:10.1029/2007JD008819.

Osterman, G., et al. (2006), Tropospheric Emission Spectrometer TES L2 data user's guide, version 2.00, 1 June 2006, report, Jet Propul. Lab., Calif. Inst. of Technol., Pasadena.

Park, M., W. J. Randel, D. E. Kinnison, R. R. Garcia, and W. Choi (2004), Seasonal variations of methane, water vapor, ozone, and nitrogen dioxide near the tropopause: Satellite observations and model simulations, *J. Geophys. Res.*, *109*, D03302, doi:10.1029/2003JD003706.

Pearson, R. W., and D. H. Stedman (1980), Instrumentation for fast response ozone measurements from aircraft, *Atmos. Tech.*, *12*, 51–55.

Richter, D. A., E. V. Browell, C. F. Butler, and N. S. Higdon (1997), Advanced airborne UV DIAL system for stratospheric and tropospheric ozone and aerosol measurements, in *Advances in Atmospheric Remote Sensing With Lidar*, edited by A. Ansmann et al., pp. 395–398, Springer, New York.

Rodgers, C. (2000), *Inverse Methods for Atmospheric Sounding: Theory and Practice*, World Sci., Hackensack, N. J.

Rodgers, C. D., and B. J. Connor (2003), Intercomparison of remote sounding instruments, *J. Geophys. Res.*, *108*(D3), 4116, doi:10.1029/2002JD002299.

Worden, H. M., et al. (2007), Comparisons of Tropospheric Emission Spectrometer (TES) ozone profiles to ozonesondes: Methods and initial results, *J. Geophys. Res.*, *112*, D03309, doi:10.1029/2006JD007258.

Worden, J. S., S. S. Kulawik, M. Shepard, S. Clough, H. Worden, K. Bowman, and A. Goldman (2004), Predicted errors of Tropospheric Emission Spectrometer nadir retrievals from spectral window selection, *J. Geophys. Res.*, *109*, D09308, doi:10.1029/2004JD004522.

M. Avery, E. V. Browell, and J. W. Hair, NASA Langley Research Center, Hampton, VA 23681, USA.

Q. Li and G. B. Osterman, Jet Propulsion Laboratory, California Institute of Technology, Pasadena, CA 91125, USA.

N. A. D. Richards, Institute for Atmospheric Science, School of Earth and Environment, University of Leeds, Leeds, LS2 9JT, UK. (n.richards@see.leeds.ac.uk)